P. N. LEBEDEV PHYSICAL INSTITUTE
USSR ACADEMY OF SCIENCES

Физический институт имени П.Н.Лебедева

F I A N

PREPRINT

37

O.D. DALKAROV, K.V. PROTASOV,
I.S. SHAPIRO

P-WAVE ENHANCEMENT IN BARYON-ANTIBARYON SYSTEMS AT LOW ENERGY

Moscow – 1988

Препринты Физического института имени П.Н. Лебедева АН СССР являются самостоятельными научными публикациями и издаются по следующим направлениям исследований Института:

- **физика высоких энергий и космических лучей**
- **оптика и спектроскопия**
- **квантовая радиофизика**
- **физика твердого тела**
- **физика космоса**
- **физика плазмы**

В библиографических ссылках на препринты Физического института имени П.Н. Лебедева мы рекомендуем указывать: инициалы и фамилию автора, номер препринта, место издания, сокращенное наименование Института-издателя, год издания.

Пример библиографической ссылки:

И.И. Иванов. Препринт 125, Москва, ФИАН, 1986.

Preprints of the P.N. Lebedev Physical Institute of the Academy of Sciences of the USSR are its independent publications and are issued in the Institute's following fields of research:

- **high energy and cosmic ray Physics**
- **optics and spectroscopy**
- **quantum Radiophysics**
- **solid state Physics**
- **cosmophysics**
- **plasma Physics**

In bibliographical references to the P.N. Lebedev Physical Institute's preprints we recommend to indicate: the author's initials and name, preprint number, place of the publication, abbreviation of the Institute-publisher, year of the publication:

Example of a bibliographical reference:

I.I. Ivanov. Preprint 125, Moscow, FIAN, 1986.

ACADEMY OF SCIENCES OF THE USSR

P. N. LEBEDEV PHYSICAL INSTITUTE

High energy physics and cosmic rays

Department of Theoretical Nuclear Physics

Preprint 37

O.D. Dalkarov, K.V. Protasov and I.S. Shapiro

P-wave enhancement in baryon-antibaryon systems at low energy

Moscow - 1988

Abstract

The physical reasons of anomalously large P-wave enhancement in $\bar{p}p$ interaction at low energy and in $\bar{p}p \to \bar{\Lambda}\Lambda$ reaction near threshold are revealed. For this the total, elastic, annihilation and charge-exchange cross-sections of $\bar{p}p$ interaction, energy dependence of real-to-imaginary ratio for forward elastic $\bar{p}p$-scattering amplitude, shifts and widths of 1S- and 2P-levels of $\bar{p}p$-atom, and also total, differential cross-sections, polarization of $\bar{\Lambda}(\Lambda)$ in $\bar{p}p \to \bar{\Lambda}\Lambda$ reaction near threshold are calculated using coupled channel model and compared with LEAR data. It is shown that the common reason of observable P-wave enhancement in all these processes is the existence of nearthreshold P-states of quasinuclear nature in nucleon-antinucleon and hyperon-antihyperon systems.

Introduction

Experimental data on $\bar{p}p$ and $\bar{\Lambda}\Lambda$ interactions which were obtained recently show up a large enhancement of P-wave in baryon-antibaryon systems near thresholds. Among them it is necessary to note the following :

(a) In the LEAR experiments the differential cross-section for $\bar{p}p$ elastic scattering at low energy was measured [1]. In Fig. 1 taken from ref. [1] the differential cross-section of $\bar{p}p$-scattering (incident $\bar{p}$ momentum in c.m. system K = 144 MeV/c) in comparison with anologous cross-section for pp-scattering at the near momentum (K = 138 MeV/c [2]) is shown. The forward peak (at the angles in c.m.s. $\theta \leq 10$) is due to Coulomb interaction. In the interval of angles $10 \leq \theta \leq 30$ the Coulomb-nuclear interference is essentially used for extraction such interaction characteristics as total cross-section, slope parameter and real-to-imaginary ratio for the forward elastic scattering amplitude. At the angles $\theta > 30$ where nuclear interaction dominates $\bar{p}p$-and pp-scatterings are distinctly differed: there is a strong forward anisotropy (rectilinearness) in $\bar{p}p$-scattering at the momenta considered above. Experimental data indicate clearly that in $\bar{p}p$-scattering at low relative momenta the contribution of partial waves with nonzero orbital momenta is large at the same time in pp-scattering S-wave dominates. A rough phase shift analysis of these experimental data reveals that P-wave contribution in the cross-section of $\bar{p}p$ elastic scattering is about 30% and about 50% in the annihilation cross-section (D-wave contribution do not exceed ~10%). The obtained values for P-wave contribution are anomalous. They are substantially higher than usual theoretical estimations according to these the ratio of L/S contributions must be of the order of $(KR)^{2L}/[(2L+1)!!]^2$ (K is c.m. momentum, R ~ ~ 1 fm is the radius of nuclear forces, L is the orbital momentum for relative motion of $\bar{p}$ and p), i.e. (if KR ≪ 1) should not exceed in this case the value of ten per cents for L = 1.

The same phenomenon was observed in the charge exchange reaction $\bar{p}p \to \bar{n}n$ even at relative momenta less than 140 MeV/c. In Fig. 2 taken from ref. [3] the differential cross-section for $\bar{p}p \to \bar{n}n$ reaction at incident antiproton momentum P = 183 MeV/c is shown. From the figure an angular anisotropy demonstrating a large P-wave contribution is clearly seen.

(b) Study of lightest antiprotonic atom - protonium indicates on the large annihilation from 2P-state. The annihilation width of 2P-state measured at LEAR is in 40 times larger than it is usually expected (from the experiment $\Gamma_{2P} \cong 40$ meV [4] instead of the of the order of 1 meV). The ratio Γ_P / Γ_{tot} from atomic experiments is in the diapason from 20% [5] to 40% [6] what is substantially higher than expected (without resonances) P-wave contribution in low energy antiproton annihilation.

(c) Another groupe of new experimental data concern to the study of energetical behaviour of the value ρ - real-to-imaginary ratio for the forward $\bar{p}p$ elastic scattering amplitude. This ratio was measured at LEAR experiments using Coulomb-nuclear interference in the diapason of incident antiproton momenta P = 180 - 600 MeV/c [7,8] and also in the works which were carried out earlier (at higher momenta) [9,10,11]. Most of published data on energy dependence of ρ are shown in Fig. 3. Besides that ρ could be extractad from $\bar{p}$-nucleus scattering data. As it was shown in ref. [12] the differential cross-section in difractive minima is very sensitive to ρ. The authors of ref. [12] using this property carried out the analysis of $\bar{p}$-nucleus scattering on nuclei from ^{12}C to ^{208}Pb. The values obtained this way are in good agreement with ρ measured directly in $\bar{p}p$-scattering.

From these data it follows that the value ρ grows down to the threshold and closes to zero at very small momenta. From the other side the measurements of the shift and width of 1S-level for protonium give a ratio $\rho \simeq 2\,\Delta E/\Gamma \sim -1$ [13,14]. Hence the value ρ has a very sharp energy dependence just near threshold at the momenta P = 0 - 200 MeV/c. As it was first mentioned in ref. [15] such very fast increasing of ρ at the momenta from 0 to 200 MeV/c could be explained by the large P-wave contribution, i.e. turned out to be directly connected with other phenomena pointed out - the effect of P-wave enhancement. (Let's mentioned that a comment in ref. [41] on the results of ref. [15] that the reason of unusual behaviour of ρ is due to openning of $\bar{p}p \to \bar{n}n$ channel only is not true and is based on misunderstanding).

(d) More expressive data which demonstrate an anomalous P-wave contribution in the interaction of slow baryons with antibaryons were obtained from the investigaton of $\bar{p}p \to \bar{\Lambda}\Lambda$ reaction at very low ($\lesssim$ 3 MeV) kinetic energies in $\bar{\Lambda}\Lambda$ system [16]. Study of the energy dependence for the cross-section of $\bar{p}p \to \bar{\Lambda}\Lambda$ reaction show up that this cross-section just near threshold (see Fig. 4) reveals K^3-dependence instead of linear K behaviour corresponding to the production of $\bar{\Lambda}\Lambda$ pair in S-state (K is a momentum in c.m. system $\bar{\Lambda}$ and Λ). Such regime is observed even at very low momenta $K \lesssim 30$ MeV/c (what corresponds to the $\mathcal{E}_{\bar{\Lambda}\Lambda}$ kinetic energy $\mathcal{E}_{\bar{\Lambda}\Lambda} \lesssim 1$ MeV). The measured angular distribution of $\bar{\Lambda}$ (Λ) is strongly anisotropic even at the momenta $K \sim 20$ MeV/c (see Figs. 5(a,b)). In the same experiments a nonzero polarization for $\bar{\Lambda}$ (Λ) at all momenta considered above was observed. This fact indicates directly on the existence of triplet P-wave in $\bar{\Lambda}\Lambda$ system (Fig. 6).

Experimental data considered above testify to substantional role of P-wave contribution in $\bar{\Lambda}\Lambda$ interaction in comparison to S-wave contribution even at K for which an expected P-wave contribution according to conventional theoretical estimations should not exceed of per cent in the considered cross-sections near threshold. If we try to explain even 10% of P-wave contribution proposing an expansion of the region for $\bar{\Lambda}\Lambda$ interaction, the radius for this region should be taken equal to one for uranium nucleus ($\sim$ 7 fm)!

The real reason for the large P-wave enhancement in $\bar{p}p$ and $\bar{\Lambda}\Lambda$ interactions at low energy is due to nuclear $\bar{B}B$ forces (B = N, Λ) which are as it is expected strongly attractive. Therefore the existence of nearthreshold (closed to 2M, where M is the mass of baryon) bound (or resonant) quasinuclear P-states are possible. Due to corresponding poles in $\bar{p}p$-scattering amplitude P-wave contribution in the scattering cross-section will be enhanced (as such as the cross-section for triplet S-wave n-p scattering is enhanced through deutron pole). As it is followed from the unitarity of manychannel S-matrix an amplitudes of all processes will have the same poles. In the case considered here this means that the annihilation cross-section at low energy will be enhanced through quasinuclear poles in the same manner as a probability of elastic scattering.

An existence of $\bar{N}N$ quasinuclear P-states was predicted 17 years ago (see refs. in the review [17]) in the framework of OBEP model. After this it was cleared up that the physical reason of angular anisotropy in $\bar{p}p$-scattering at low energy is a nuclear interaction [18] but not annihilation taking into account of which many authors tried to explain distinct difference between $\bar{p}p$- and pp-scatterings at low energy . It is necessary to note that the experimental data on P-wave contribution in $\bar{p}p \rightarrow \bar{\Lambda}\Lambda$ reaction considered above show that the P-wave enhancement effect in $\bar{p}p \rightarrow \bar{\Lambda}\Lambda$ processes is unlikely due to annihilation. The main contribution into this reaction is given by the strange meson exchange, just as the role of mesonic annihilation with the following reannihilation into $\bar{\Lambda}\Lambda$ pair is negligible. At the same time the expansion of annihilation radius up to needed size ($\sim$7 fm) looks physically inadmissible. The unique real basis for the explanation of available experimental data on large P-wave enhancement in baryon-antibaryon systems at low energy is an existence of nearthreshold poles.

However it was always clear (this question was discussed in the first theoretical works (see ref. [17])) that main problem of theory consists in the correct estimation of influence on the positon of nearthreshold levels and in the calculation their annihilation widths.

Since the annhilation cross-secton at low energy is closed to the unitary limit it seems on the face of it that annihilaton widths should be large also and P-wave enhancement proposed above will not operate. In the reality annihilaton cross-section turns out to be large (closed to unitary limit) exactly owing to the smallness of annihilation level width since in this case the resonant enhancement is large. The physical reason for narrow widths is due to the fact that from physical point of view an annihilation distances should be equal (by the order of magnitude) to Compton wave length of annihilating particles ($\sim$ 0.1 fm), i.e. should be small in comparison with the radius of bound quasinuclear state ($\sim$ 1 - 2 fm) (the same situation is well known in the theory of hadron atoms: level shifts and widths are small because strong hadron-nuclear interaction acts only on the distances much less than atomic Bohr radius). The first rough estimations for annihilation widths of quasinuclear levels (see [17]) grounded on factorization relation (like the formulae for hadron atoms) give the values for the widths in the diapason between 1 - 100 MeV in dependence on orbital momenta. After the validity of factorization relation in the framework of coupled channel model (CCM) [19,20] was studied.

In this work we use a coupled channel model for the description of recently obtained experimental data on $\bar{p}p$ and $\bar{\Lambda}\Lambda$ interactions at low energy. Our purpose is to find out the physical nature of P-wave enhancement effects in the scattering and annihilation of slow antiprotons and in $\bar{p}p \rightarrow \bar{\Lambda}\Lambda$ reaction near threshold. It will be shown that the reason for anomalous P-wave contribution in $\bar{p}p$- and $\bar{\Lambda}\Lambda$-interactions at low energy is the presence of nearthreshold bound and resonant P-states in the considered baryon-antibaryon systems. Some of the results contained in this work were published earlier as short communications [22].

The scheme of the exposition is as follows. In section 2 we formulate simple CCM for description of the experimental data on $\bar{p}p$-interaction. Section 3 is devoted to the formulation of CCM for simultaneous description of $\bar{B}B$ systems and to discussion of main properties of CCM which are needed for description of the experimental data on $\bar{p}p$- and $\bar{\Lambda}\Lambda$-interactions. In section 4 the results of numerical calculations for $\bar{p}p$ elastic, charge-exchange and annihilation cross-sections are given and are compared with the experimental data. Also the spectrum of quasinuclear P- and D-states in $\bar{N}N$ system is shown. The real-to-imaginary ratio for $\bar{p}N$ elastic scattering amplitude is considered in section 5. In section 6 the $\bar{p}N$ scattering lengths in S- and P-states and also the shifts and widths of S- and P-protonium levels are calculated. The section 7 is devoted to the calculation of total cross-section, differential cross-section and polarization $\bar{\Lambda}$ (Λ) in the $\bar{p}p \to \bar{\Lambda}\Lambda$ reaction. It will be shown that observed phenomena are caused by the presence of quasinuclear P-resonance in $\bar{\Lambda}\Lambda$ system. In conclusion the main consequences and results obtained in this work are summarized.

2. Simple two channel model

The main peculiarity of this model which has been used earlier (see refs. [20,21]) is simplistic phenomenological treatment of nucleon-antinucleon annihilation. The channel 1 here corresponds to $\bar{N}N$ system. An interaction between $\bar{N}$ and N is due to one boson exchange which is described by the potential [23] V_{OBEP} = = V_{11}. The simplistic treatment of annihilation is that all of numbers of different $\bar{N}N$ annihilation channels are replaced by the only one (channel 2). This channel contains two noninteracting particles. Here as earliar in ref. [21] the mass of each this particle is putted on the mass of ρ-meson: M_2 = 763 MeV. The coupling of 1 and 2 channels is realized by short range Yukawa potential

$$V_{12} = \lambda_L \cdot \frac{e^{-r/r_a}}{r} , \qquad (1)$$

where r_a is the annihilation radius, λ_L is the dimensionless constant which is depend on orbital momentum for $\bar{N}$ and N relative motion. Isospin and G-parity of particles in the 2 channel are not fixed also owing to there are no any specific limitation for

$\bar{N}N$ annihilation from different spin and isospin states. Actually this means that in our model many two particles noncoupled (due to the difference of conserved quantum numbers) channels are proposed. However the formalism for calculation in this model is identical to the method of the solving of two channel task. Its dynamical ground is the potential matrix

$$V = \begin{pmatrix} V_{11} & V_{12} \\ V_{12} & 0 \end{pmatrix} \qquad (2)$$

This is Hermitian matrix since V_{11} and V_{12} are real in consequence of that S-matrix is unitary in CCM (unlike a scattering S-matrix in optical model with complex potential an imaginary part of which takes into account annihilation processes).

Analitical properties of S-matrix in two channel CCM as a function of energy were considered in ref. [20]. Here we would like first of all to study the dependence of annihilation cross-section σ_{ann} on coupling constant λ. The point is that as it was shown in ref. [20] the same annihilation cross-section σ_{ann} could be obtained for different values of λ even for simplest case - separable potential V_{12} (see fig.7). In connection witn this a question is what λ corresponding to observable σ_{ann} is physically justified. The answer on this question demands an investigation of the function $\sigma_{ann}(\lambda)$ for realistic local potentials.

Such study was carried out in present paper for potential (1) (numerical calculations). In fig.8 the dependence obtained is shown. Annihilation cross-section $\sigma_{ann}(\lambda)$ has oscillating behaviour as a function of λ. Such behaviour of $\sigma_{ann}(\lambda)$ could be obtained analytically for local potential choosing potential as a square well. Function $\sigma_{ann}(\lambda)$ is written in Appendix I.

From the results discussed above it follows that many different values for coupling constant correspond to the same annihilation cross-section for local realistic potentials. For this reason the choice of annihilation coupling constant in the interaction Hamiltonian for CCM is very essential in wording of the problem. In this model the main qualitative characteristic - annihilation shortrangeness as compared with nuclear forces (annihilation radius r_a in (1) is equal of the order of magnitude to Compton wave length of baryon) is taken into account only. To the opinion of the authors a modern status of theory do not support the possibility to calculate without perturbation arguments an annihilations effects in baryon-antibaryon interaction taking into account a details of annihilation dynamics which is really relativistic quantum field process. On the other hand the nuclear interaction of slow antibaryons with baryons could be considered more universal in the framework of potential approach which is used successfully in the description of nonrelativistic baryon systems (including nuclei). Hence the theory of nonrelativistic baryon-antibaryon systems grounded on any phenomenological CCM will have a physical sence only in the case if the observable consequences will depend weakly on the details of annihilation processes. This is possible due to the smallness of annihilation radius as compared with nuclear forces one at limited value of annihilation constant λ considered above. At very large λ the forces corresponding to virtual annihilation as it is shown in the following diagram begin to act:

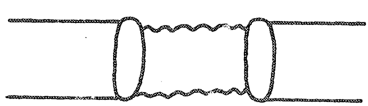

(3)

This "annihilation scattering" at sufficiently large λ could change a wave function at the distances of the order of nuclear forces. A criterium of smallness this changing which is needed as it was shown in [20] is a factorization relation of annihilation cross-section on nuclear and annihilation parts.

After that as it was shown in ref. [20] the factorisation is realized at $\lambda < \lambda_{max}$ (i.e. at left side of "hump"- see fig.7). It could be expected that for local interaction the factorization takes place at $\lambda < \lambda_{1\ max}$ also. Therefore a constant λ for description of experimental data on $\bar{p}p$-interaction should be in the diapason between 0 and $\lambda_{1\ max}$. This condition was not reached in ref. [21], but it is valid in this paper.

In this model two sets of parameters are exist, one of them corresponds to annihilation, second - to nuclear interaction.

As it was noted above the interaction for transition from channel 1 to 2 was taken in the form (1), where r_a is the annihilation radius which is equal to $r_a \sim 1/2M_N$ (M_N is the nucleon mass) [17], in concrete calculations it was chosen $r_a = 1/1.85M_N$ (as in ref. [21]). The dimensionless constant λ_L should be valid to two conditions: 1) λ_L is in the diapason from 0 to $\lambda_{1\ max}(L)$; 2) it is necessary to support an observable annihilation cross-section. In $\bar{N}N$ scattering for the energy range from $\bar{N}N$ threshold (1878 MeV) to E $\simeq$ 1950 MeV S-, P-, and D-waves take into participation for which λ_L was taken:

$$\lambda_S \simeq 4, \qquad \lambda_P \simeq 18, \qquad \lambda_D \simeq 44.$$

The realistic one boson exchange potential has a singularity at small distances therefore it is necessary to do a regularization which was realized by zero cut-off

$$V_{11}(r) = 0 \quad \text{at} \quad r < r_c$$

since r_c depends on quantum numbers of the system in this task r_c was chosen to get first of all a correct value for annihilation cross-section for $\bar{p}p$-interaction. The rest values experimentally observed (elastic, charge-exchange cross-sections, real-to-imaginary ratio for the forward elastic scattering amplitude) are recieved automatically. The values of r_c are shown in Table 1 (in fm).

For simplification of calculations tensor forces leaded to the mixing of the states with L = J ± 1 were asided.

3. Model for calculation of $\bar{p}p \rightarrow \bar{\Lambda}\Lambda$ process

Considerable problem in $\bar{N}N$ scattering is the taking into account the hyperon-antihyperon channels. Here we propose a method to take into consideration the channels with strange particles (Λ or Σ) in the presence of annihilation.

First simplest and on a glance correct approach is in the following: two channel task (annihilation channel and $\bar{N}N$ one) turns into four channel for isospin 0 (annihilation, $\bar{N}N$, $\bar{\Lambda}\Lambda$, $\bar{\Sigma}\Sigma$) or five channel for isospin 1 (annihilation, $\bar{N}N$, $\bar{\Lambda}\Sigma$, $\Lambda\bar{\Sigma}$, $\bar{\Sigma}\Sigma$). Between them baryon-antibaryon channels are connected by the OBEP. All of three (or four for isospin 1) channels with strong interacting particles are connected with annihilation channel. Moreover annihilation couplings and annihilation radii r_a for all channels would not drastically distinguished (for simplicity they were putted on equal). In this scheme a potential has the form (for isospin 0, for 1 - analogically):

$$V = \begin{pmatrix} 0 & V_{ann} & V_{ann} & V_{ann} \\ V_{ann} & & & \\ V_{ann} & & \text{OBEP} & \\ V_{ann} & & & \end{pmatrix} \qquad (.)$$

where V_{ann} is the annihilation potential (by the assumption the same for all channels). "OBEP" is the matrix 3 × 3 (for isospin 0) or 4 × 4 (for isospin 1) of OBE potentials.

We are interesting for influence of $\bar{Y}Y$ channels on annihilation $\bar{N}N$ cross-section. Let's consider sufficiently low energies closed to $\bar{N}N$ threshold in the range E = 1880 - 1950 MeV.

From the begining the influence of $\bar{Y}Y$ channels due to OBEP is considered. This will make using $\bar{\Lambda}\Lambda$ channel since this one lies more close to $\bar{N}N$ threshold therefore this channel proves to be most influence. An effective interaction potential in $\bar{N}N$ channel taking into account $\bar{\Lambda}\Lambda$ channel will have the form (symbolically):

$$V^{eff}_{\bar{N}N} = V_{\bar{N}N} + V_{N\Lambda} G_{\bar{\Lambda}\Lambda} V_{N\Lambda} \qquad (5)$$

where $V_{\bar{N}N}$ is the interaction in $\bar{N}N$ channel without $\bar{\Lambda}\Lambda$ channel, $V_{N\Lambda}$ is the transition potential from $\bar{N}N$ to $\bar{\Lambda}\Lambda$ channel, $G_{\bar{\Lambda}\Lambda}$ is the exact Green function in $\bar{\Lambda}\Lambda$ channel. If for this Green function the spectral representation is used it will be clear that the main contribution in $V^{eff}_{\bar{N}N}$ potential corresponds to the lowest bound state in $\bar{\Lambda}\Lambda$ system, since its contribution in the spectral density is proportional to $\sim 1/(E_n - E)$, where E is the energy for scattering problem (this value is of the order of 1900 MeV), E_n is the energy of this state (all states in system are closed to $\bar{\Lambda}\Lambda$ threshold i.e. $2M_{\Lambda}$ = 2231 MeV [25]). Hence due to the factor $1/(E_n - E)$ a contribution of the second term in formula (5) turns to be small. Second term will be essential in $\bar{N}N$ scattering only at the energy $E \sim 2$ GeV.

For this reason at the energy $E \sim 1900$ MeV the small components in potential (4) (i.e. matrix elements of OBEP which are correspond to $\bar{Y}Y$ channels and $\bar{N}N \rightarrow \bar{Y}Y$ transitions) could be excluded. In consequence the potential is obtained in the following form (for isospin 0):

$$V = \begin{pmatrix} 0 & V_{ann} & V_{ann} & V_{ann} \\ V_{ann} & V_{\bar{N}N} & 0 & 0 \\ V_{ann} & 0 & 0 & 0 \\ V_{ann} & 0 & 0 & 0 \end{pmatrix}$$

As it was noted above it is better to work with annihilation constants λ for which the factorization of annihilation cross-section is realized. Therefore it is sufficient to study $\sigma^{ann}_{V_{\bar{N}N}=0}$. Moreover in this region a separable interaction should reproduce all to our interest. For obtaining of analytical form one will be considered that the potential has the following separable form:

$$V = V_0 |\xi><\xi| \equiv \begin{pmatrix} 0 & 1 & 1 & 1 \\ 1 & 0 & 0 & 0 \\ 1 & 0 & 0 & 0 \\ 1 & 0 & 0 & 0 \end{pmatrix} \cdot |\xi><\xi|$$

One could ever consider that potential matrix has arbitrary dimension N × N. Then the scattering amplitude T in Lippman-Schwinger equation

$$T = V + V G_0 T$$

(G_0 is the free Green function) will be find in the form $T = F \cdot |\xi><\xi|$.

For F algebraic equation is obtained which can be easily resolved:

$$F = (1 - V_0 <\xi|G_0|\xi>)^{-1} \cdot V_0$$

F_{12} element of F matrix which is contained in the expression for annihilation $\bar{N}N$ cross-section (cross-section for transition between 1 and 2 channels) is in the interest.

$$\sigma^{ann}(\lambda) \sim \frac{K'}{K} \cdot |F_{12}|^2 \cdot |<\xi|\vec{K}><\vec{K}'|\xi>|^2$$

where $\vec{K}'$ is the relative momentum for the particles in channel 1, $\vec{K}$ is the same for channel 2. F_{12} element is easily calculated. In consequence

$$\sigma^{ann}(\lambda) \sim \frac{\lambda^2}{\left| 1 - \lambda^2 g_{\xi 1 \xi} \sum_{i=2}^{N} g_{\xi i \xi} \right|^2}$$

where $g_{\xi i \xi} \equiv <\xi|g_i|\xi>$, g_i is the free Green function for channel i, i = 1 ÷ N.

The graph of this function is shown in fig. 7. Maximum of the curve corresponds to

$$\lambda_{max} = \frac{1}{\sqrt{\left| g_{\xi 1 \xi} \sum_{i=2}^{N} g_{\xi i \xi} \right|}}$$

Let $g_{\xi 2 \xi} \simeq g_{\xi 3 \xi} \simeq \dots \simeq g_{\xi N \xi} = g_{\xi}$ (the validity of this assumption for many channel problem with realistic nucleon and hyperon masses will be discussed later), then

$$\lambda_{max} \sim \frac{1}{\sqrt{N-1}} \frac{1}{\sqrt{| g_{\xi 1 \xi} \cdot g_{\xi} |}}$$

and annihilation cross-section at $\lambda = \lambda_{max}$ will be

$$\sigma_{ann} (\lambda = \lambda_{max}) \sim \frac{1}{N_{bar}}$$

where N_{bar} = N - 1 is the number of baryons considered here.

Hence the simplest estimations show that the first maximum of annihilation cross-section is displaced in $\sqrt{N_{bar}}$ times and its value in the first maximum is decreased at N_{bar} times. Note that numerical calculation fulfield for realistic potentials is fairly agreed with these estimations. The dependence of $\sigma_{ann}(\lambda)$ for Yukawa type potential was obtained the same as in fig. 8 and besides $\lambda_{max\ 1} \simeq 2$ and $\sigma_{ann}(\lambda)/\sigma_{UL} \simeq 5\%$ (σ_{UL} is the unutary limit for σ_{ann}). For two channel case: $\lambda_{max\ 2} \simeq 4$ and $\sigma_{ann}(\lambda)/\sigma_{UL} \simeq 20\%$.

Now it is necessary to understand: 1) why is true the qualitative estimations for separable interaction in many channel case (i.e. an assumption $g_{\xi 2 \xi} \simeq \dots \simeq g_{\xi N \xi}$ which is seems to be doubtful at a glance); 2) what is the correct method for the taking into account more high-lying channels for $\bar{N}N$. It is clear that the method considered above is not valid since the introducing of new channels diminishes automatically the annihilation cross-section ¬ nucleon-antinucleon system even if these additional channels should not yet have influence on $\bar{N}N$ system according to the estimations (5) for nuclear interaction.

For answer the first question let's consider $|\xi\rangle$ in the form $\langle \vec{r}|\xi\rangle = \sqrt{\beta/2\pi}\cdot e^{-\beta/r}/r$ (this form $|\xi\rangle$ is more closed to the case of local potential considered here). Then for $g_{\xi i \xi}$ one obtain $g_{\xi i \xi} \sim \beta^2/(K_i + i\beta)^2$, where K_i is the momentum in channel i. Here $\beta \sim \sim 2M_N$ just as at the considered energies $|K_i| < 500$ MeV/c (for channels $\bar{N}N$, $\bar{\Lambda}\Lambda$, $\bar{\Lambda}\Sigma$, $\Lambda\bar{\Sigma}$, $\bar{\Sigma}\Sigma$). This means that an assumption $g_{\xi 2 \xi} \simeq \simeq \ldots \simeq g_{\xi N \xi}$ is so much the better as smaller parameter K_i/β. From physical point of veiw this means that at small distances (where baryon and antibaryon draw together up to the distances of the order of annihilation radius - very small value - about 0.1 fm) the particle has such momentum (virtual) that the mass difference for nucleon and hyperon will turn to be negligible. It is seen that such method for the taking into account $\bar{N}N$ annihilation (in the presence of $\bar{Y}Y$ channels) leads to the disappearence of mass difference between nucleon and hyperon. From the other side it is known that among $\bar{N}N$ annihilation products the channels with strange particles is about 5% [26], just as for $\bar{\Lambda}\Lambda$ one could expect that annihilation into $\bar{K}K$ +etc will dominate i.e. $\bar{N}N$ and $\bar{\Lambda}\Lambda$ annihilation channels are not coincided.

It is clear from considered above that nucleon-antinucleon scattering taking into account hyperon-antihyperon channels should be considered in the following way: each baryon-antibaryon channel ($\bar{N}N$, $\bar{\Lambda}\Lambda$, $\bar{\Lambda}\Sigma$ and $\Lambda\bar{\Sigma}$, $\bar{\Sigma}\Sigma$) would have its annihilation channel and different baryon-antibaryon channels would be connected to each other by transition OBE potential. For simplicity one could propose that in annihilation channels the particles are free and an interaction between annihilation channels does not exist. Now in the limit where coupling between different baryon-antibaryon channels goes to zero the task is desintegrated on several independent ones in each of which a scattering of corresponding particles taking into account of annihilation is considered. In particular we obtain automatically two channel case for $\bar{N}N$ system at the energy E $\sim$ 1900 MeV.

According to the considered above let's make a model for description new experimental data for $\bar{p}p \rightarrow \bar{\Lambda}\Lambda$ reaction at the energy in $\bar{\Lambda}\Lambda$ c.m. system $\varepsilon_{\bar{\Lambda}\Lambda}$= 0 - 6 MeV above $\bar{\Lambda}\Lambda$ threshold. A model is actually two of two channel systems connected together: first two channels correspond to $\bar{N}N$ and annihilation channel for $\bar{N}N$ (these two channels were defined in section 2); other two channels correspond to $\bar{\Lambda}\Lambda$ and annihilation one for $\bar{\Lambda}\Lambda$. Channels $\bar{N}N$ and $\bar{\Lambda}\Lambda$ are connected together by OBEP corresponded to K and K^*-meson exchange. Coupling constants of K and $K^*$with $\bar{N}$ and $\bar{\Lambda}$ were taken as $g_{K\bar{N}\bar{\Lambda}} = -g_{KN\Lambda}$ and $g_{K^*\bar{N}\bar{\Lambda}} = g_{K^*N\Lambda}$. In accordance with the assumption considered above $\bar{N}N$ and $\bar{\Lambda}\Lambda$ annihilation channels are not connected.

All of parameters for $\bar{N}N$ system: annihilation radius r_a annihilation coupling constant λ_L, mass of particles in annihilation channel, cut-off radii for nuclear $\bar{N}N$ potential were fixed earlier (see section 2). It is necessary now to fix also analogous parameters for $\bar{\Lambda}\Lambda$ system and cut-off radii for $\bar{N}N \rightarrow \bar{\Lambda}\Lambda$ transition potential.

Since from the experimental data for $\bar{\Lambda}\Lambda$ system are nothing known we make this in the following way. By the analogy with $\bar{N}N$ system: annihilation radius was taken $r_a(\bar{\Lambda}\Lambda) = 1/2M_\Lambda \simeq 0.09$ fm M_Λ is the mass of Λ-hyperon; annihilation constants for $\bar{\Lambda}\Lambda$ system were taken the same as in $\bar{N}N$ system (at the energies consid ered above the contributions of S- and P-waves are considered only) i.e. $\lambda_S(\bar{\Lambda}\Lambda) = \lambda_S(\bar{N}N)$, $\lambda_P(\bar{\Lambda}\Lambda) = \lambda_P(\bar{N}N)$; mass of particles in annihilation channel for $\bar{\Lambda}\Lambda$ was taken equal to K^*-meson one. Such choice of the mass in annihilation channel is due to the purpose to make similar an annihilation in $\bar{N}N$ and $\bar{\Lambda}\Lambda$ systems: in this case we obtain $M_\Lambda/M_N \simeq M_{K^*}/M_\rho$ and from other side first maximum in annihilation cross-section $\sigma_{ann}(\lambda)$ lies at approximately the same values of λ as in $\bar{N}N$ system. Cut-off radii for nuclear interaction in $\bar{\Lambda}\Lambda$ channel were taken from ref. [25] (all of cut-off radii r_c = 0.64 fm).

Hence the only one free parameter which was used to fit total cross-section of $\bar{p}p \to \bar{\Lambda}\Lambda$ reaction is cut-off radius r_c for transition potential $V(\bar{p}p \to \bar{\Lambda}\Lambda)$. For description of experimental data the following cut-off radii were used: $r_c(^1S_0)$ = 0.67 fm, $r_c(^3S_1)$ = 0.7 fm, $r_c(^3P_0) = r_c(^1P_1) = r_c(^3P_1) = r_c(^3P_2)$ = 0.96 fm. It is not so important that the values of these parameters are relatively large (as compared with cut-off radii for diagonal $\bar{N}N$ and $\bar{\Lambda}\Lambda$ potentials). The point is that coupling constants for K and K^*-mesons are known very bad therefore they could be considered as the variable parameters, but we have prefered to fix the constants $g_{K\bar{N}\bar{\Lambda}}$ and $g_{K^*\bar{N}\bar{\Lambda}}$ corresponding to $g_{KN\Lambda}$ and $g_{K^*N\Lambda}$ from the description of the data in baryon-baryon channel [23] and to varify cut-off radii for transition $\bar{N}N \to \bar{\Lambda}\Lambda$ potential.

4. Comparison with experimental data

In considering a comparison of the obtained theoretical results with experimental data it is necessary to note that CCM is very simple model putted in a claim for description of the main qualitative properties of the problem under discussion. For this reason it is not necessary to attach importance to possible divergence between quantitative details of model calculations and experimental data.

The results of the calculations of total (σ_{tot}) and annihilation (σ_{ann}) cross-sections for $\bar{p}p$-interaction are shown in figs. 9 and 10 correspondingly. Theoretical results for partial annihilation cross-sections for S-, P-, and D-waves are represented in fig 11. Fast increasing and large contribution of P-wave at low momenta are clearly seen. Momentum K = 144 MeV/c in c.m.s. corresponds to the experiment [1] fulfield at CERN and cited above. P-wave contribution in annihilation cross-section is equal to $\sigma_{ann}(P)/\sigma_{ann} \cong 75\%$ at this momentum. In fig. 12 the energy dependence of elastic (σ_{el}) and charge exchange ($\sigma_{\bar{p}p\to\bar{n}n}$) cross-sections is shown. Effect of P-wave enhancement leads to the dip in theoretical curve for σ_{el} at $E_{cm} \cong$ 1880 MeV which as it seems to us is in agreement with experimental data (though experimental errors are large yet). As it was expected the total P-wave contribution into elastic cross-section σ_{el} turns to be large. At the momentum K = 144 MeV/c about 50% of σ_{el} is given by P-wave as it is demonstrated in fig. 13. An interference of S- and P-waves leads to the large observable forward anisotropy for the angle distribution (in c.m.s.) of scattered $\bar{p}$ (calculated differential cross-section of $\bar{p}p$-scattering is shown in fig. 14). To avoid a mistake in the understanding that annihilation is a real reason for P-wave enhancement we have calculated S- and P-wave contributions to σ_{el} when annihilation is turned off ($\lambda_L = 0$) but OBEP is taken into account. The results are shown in fig. 15. It is seen that in this case P-wave contribution is even more achieving 80% instead of 50% when annihilation is included. This phenomenon (first emphasized in ref. [18]) as it was noted above demonstrates clear that P-wave enhancement is caused by the nuclear $\bar{N}N$ interaction but not the openning of annihilation channels.

The explanation of the physical nature of P-wave enhancement considered above is contained in Table 2. There the results of calculations for nearthreshold bound and resonant states in CCM are shown. As we can see from Table 2 there are 5 nearthreshold P-levels which (as it is followed from our calculations) give the main part of P-wave enhancement of annihilation and elastic cross-sections. These levels considered as the poles of S-matrix are decisive for all amplitudes of $\bar{p}p$-interaction at threshold.

5. Real-to-imaginary ratio for the forward elastic $\bar{p}N$ scattering amplitude

The experimental data reveal very fast growth of the ratio ρ with increasing of $\bar{p}$ momentum in c.m.s. from $P = 0$ to 200 MeV/c (see fig.3). As it was first shown in ref. [15] the rapid rise of ρ with increasing of $\bar{p}$ momentum could be explained in the assumption of large P-wave in this region. The results of CCM calculations shown in fig. 16 confirm this observation. As it can be seen on figure the CCM calculations reproduce the main feature of the P-dependence of the quantity ρ at low momenta. Qualitatively, the effect of rapid rise of ρ consist in the opposite signes of S- and P-wave amplitudes of $\bar{p}p$ elastic forward scattering therefore a large contribution and rapid rise of P-wave amplitude leads to the compensation of real parts of S- and P-amplitudes i.e. to zero values of ρ at the momenta $P \lesssim 300$ MeV/c. In our calculations of ρ we did not take into account the Coulomb effects which can increase ρ by the absolute value at $P = 0$ approximately on 10% (at $P \simeq 300$ MeV/c Coulomb corrections are negligible). At the same time it is necessary to note that the extraction of ρ from $\bar{p}p$ data in the region of Coulomb-nuclear interference should realized using correct formula for such interference [27]. This can decrease ρ at $P \lesssim 200$ MeV/c on the value of the order of $\Delta\rho \sim 0.05$ that leads to better agreement between experimental results and theoretical curve in fig. 16.

Effect of rapid rise of P-wave contribution is revealed more clearly in the dependence of ρ for the amplitude with pure isospin state $I = 1$ i.e. for $\bar{p}n$ (or $\bar{n}p$) scattering (see fig. 17). Now an extraction of ρ in pure isospin state $I = 1$ is possible only from the data on $\bar{p}$-nucleus scattering (see refs. [12,28]). The value ρ obtained in ref. [28] at $\bar{p}$ momentum ~ 600 MeV/c in laboratory system as it is seen on fig. 17 are not in disagreement with our calculations.

6. S- and P-wave scattering lengths. Shifts and widths of S- and P-levels of $\bar{p}p$-atom

Simultaneously with the description of $\bar{p}p$-scattering data we have calculated low-energy parameters of $\bar{p}N$ scattering for S- and P-waves. S-wave scattering lengths α and real-to-imaginary ratio ρ for $\bar{p}N$ forward scattering amplitude at zero energy are shown in Table 3 (see also fig. 16). The value $\rho^{*}_{\bar{p}p}(0) = -1.08$ corresponds to slightly different dimensionless anihilation constant λ_S ($\lambda_S = 4.0$ instead $\lambda_S = 3.9$ in the partial wave $^{11}S_0$) that is not lead to any changing of the obtained results for cross-sectios at E_{cm} > 1890 MeV. It is necessary to note that taking into account of $\bar{p}p \to \bar{n}n$ threshold in $\bar{p}p$-scattering using the method of ref. [15] (see also fig. 14) one can support an increasing of $\rho_{\bar{p}p}(0)$ approximately on 10% by the absolute value. Besides that Coulomb corrections increase also the absolute value of $\rho_{\bar{p}p}(0)$ on ~ 10 %. Taking into account all of these corrections $\rho_{\bar{p}p}(0)$ has the following values: $\rho_{\bar{p}p}(0) \sim 0.9$ and $\rho^{*}_{\bar{p}p}(0) \sim 1.3$.

There are no experimental data for $\rho_{\bar{p}n}(0)$ at present. But the estimation $\mathrm{Im}\, a_{\bar{p}n}$ = 0.235±0.121 fm obtained from the data on annihilation of stopped $\bar{p}$ in ^{4}He (see ref. [30]) is in agreement with the value $\mathrm{Im}\, a_{\bar{p}n}$ = 0.28 seen in Table 3.

The shifts and widths of 1S-level of protonium calculated using S-wave scattering lengths from Table 3 turn out to be equal:

$$\underset{(\mathrm{KeV})}{\mathrm{Re}\,(\Delta E_{1S})} = \begin{matrix} 0.68 \\ \\ 0.74^{*} \end{matrix} \, , \qquad \underset{(\mathrm{KeV})}{\Gamma_{1S}} = \begin{matrix} 1.79 \\ \\ 1.39^{*} \end{matrix}$$

These values are not in disagreement with available (rather contradictory) data on the shift and width of 1S-level of $\bar{p}p$-atom.

P-wave scattering volume for $\bar{p}p$-scattering are shown in Table 4. In this case the calculated shift and width of 2P-level for $\bar{p}p$-atom is equal to:

$$\mathrm{Re}\,(\Delta E_{2P}) = -\,18 \text{ meV} \qquad \Gamma_{2P} = 39 \text{ meV} .$$

The value for Γ_{2P} obtained in our calculations is in rather good agreement with large experimental value of 2P-level width of $\bar{p}p$-atom: Γ^{exp}_{2P}= (39.8 ± 10.7) meV [4].

It is necessary to emphasize that the comparison with analogous calculations in optical models [29] shows an essentially large value of the real part of P-wave scattering length obtained in our calculations (Re A_p is about of 3 times larger then the same value in ref. [21]). Broadering of P-level in our calculations is caused as it was repeatedly noted by the existence of spectrum of quasinuclear P-wave nearthreshold $\bar{N}N$ resonances.

7. Nearthreshold P-wave enhancement in $\bar{p}p \to \bar{\Lambda}\Lambda$ reaction

The calculated total cross-section of $\bar{p}p \to \bar{\Lambda}\Lambda$ reaction is shown in fig. 18 (solid curve). It is seen that at the momentum range K ~ 50 ÷ 60 MeV/c ($\mathcal{E}_{\bar{\Lambda}\Lambda} \simeq 3$ - 4 MeV) P-wave contribution is about one half of total cross-section. The calculated differential cross-section for the reaction at kinetic energy in $\bar{\Lambda}\Lambda$ system $\mathcal{E}_{\bar{\Lambda}\Lambda}$ = 3.8 MeV in comparison with experimental data is shown in fig. 19. It is necessary to note that the model parameters (cut-off radii for $\bar{p}p \to \bar{\Lambda}\Lambda$ transition potential) were fixed using only the values of total cross-sections for $\bar{p}p \to \bar{\Lambda}\Lambda$ reaction.

The calculation of $\bar{p}p \to \bar{\Lambda}\Lambda$ total, differential cross-sections and polarization at the energy of several tens MeV were fulfield in refs. [33, 34, 35, 36].

A large P-wave enhancement in $\bar{\Lambda}\Lambda$ system observed in the experiment and calculated in our model should be caused by the same reasons as in $\bar{p}p$-interaction near $\bar{N}N$ threshold. For revealing of this question we have investigated simultaneously a spectrum of P-wave quasinuclear $\bar{\Lambda}\Lambda$ resonances. One of the P-states ($^3P_1$) which contributes substantional input to P-wave amplitude in $\bar{\Lambda}\Lambda$ system for $\bar{p}p \to \bar{\Lambda}\Lambda$ reaction has the following parameters: M =

= 2237 MeV, Γ_{tot}= 8 MeV, Γ_a= 2.5 MeV, $\Gamma_{\bar{\Lambda}\Lambda}/\Gamma_{tot}$ = 0.7, $J^{PC} = 1^{++}$. Such states could be manifest themselves as the narrow resonances in $\bar{K}K + n\pi$ systems. The cross-sections for these resonances are of the order of several μb (experimental upper limit available now for such states in $\bar{p}p \to \bar{K}K$ channel [31] is more than expected value of the cross-section). In fig. 20 the calculated polarization $\bar{\Lambda}(\Lambda)$ in $\bar{p}p \to \bar{\Lambda}\Lambda$ reaction is shown. Observation of nonzero polarization on the experiment should testify of the existence of triplet P-states in $\bar{\Lambda}\Lambda$ system.

Hence a proposed model describes besides $\bar{N}N$ channel also the main qualitative properties of $\bar{p}p \to \bar{\Lambda}\Lambda$ process. As a natural consequence the model predicts an existence of the spectrum of quasinuclear (bound or resonant) $\bar{\Lambda}\Lambda$ states. The presence of the states with nonzero orbital momenta (P-states in our case) leads to expected effect of P-wave enhancement in $\bar{p}p \to \bar{\Lambda}\Lambda$ reaction at low relative momenta of $\bar{\Lambda}$ and Λ. Analogous behaviour for the cross-sections should be observed for other channels with hyperon-antihyperon pair production, i.e. $\bar{p}p \to \bar{\Lambda}\Sigma(\Lambda\bar{\Sigma})$, $\bar{\Sigma}\Sigma$.

Conclusion

The main developments presented above show that the baryon-antibaryon interaction at low energy is determined dominantely by nuclear forces. This is caused by two factors: by the existence of nearthreshold quasinuclear levels in $\bar{B}B$ system and because of the short range of the annihilation interaction. From the physical point of view both reasons are natural and transparent. It seems that the low energy P-wave enhancement effects discussed in this paper may be considered as a strong manifestation of nearthreshold quasinuclear states.

Let us emphasize that the observed angular anisotropy in the $\bar{p}p \to \bar{\Lambda}\Lambda$ reaction just near threshold hardly can be explained as a result of S-wave suppresion in the $\bar{B}B$ interactions at low energies whereas the P-wave contribution has its normal value (as it was supposed in ref. [34]). From the dinamical point of view for the S-wave suppression the L-independent forces or annihilation in S-state must be strongly reduced. We do not see physical reason for introducing such an exotic supposition into any realistic model of the interaction responsible for the process in question. Moreover, we have learnt from the experiment that the same phenomenon (angular anisotropy) takes place in $\bar{p}p$ elastic and charge-exchange scattering ($\bar{p}p \to \bar{n}n$) at low energies, whereas the S-wave $\bar{p}p$-scattering length has its normal value. It follows from all these facts that a common property for $\bar{B}B$ interactions at low energies is rather the P-wave enhancement but not the S-wave suppression. The physical reason for the P-wave enhancement effect seems to be clear: it takes place because of the appearence of the P-wave bound or resonant nearthreshold states in the $\bar{B}B$ systems which are caused by strong attraction forces acting between $\bar{B}$ and B. All realistic OBEP models give such forces and the annihilation processes as it was shown above do not destroy the results of nuclear interaction because the annihilation range is much smaller than the nuclear one.

The used coupled channel model does not pretend to give an exact position of quasinuclear levels and their widths mainly because the annihilation was treated very roughly. But it seems the P-wave $\bar{B}B$ bound states would expected really to have the widths about 30 - 80 MeV. For this case the calculations of the discrete γ-spectrum corresponding to the $(\bar{p}p)_{atom} \to (\bar{N}N)_{nucl}$ transitions was performed long time ago in ref. [32]. The theoretical estimations [32] gave for the relative probability of the transitions between S-levels of $\bar{p}p$-atom and quasinuclear P-states the values in the range (0.4 - 5.0)$\cdot 10^{-3}$(a ratio $\Gamma_\gamma / \Gamma_{ann}$ was calculated, where Γ_{ann} is the annihilation width of atomic 1S-level, Γ_γ is the radiative width of the transition). For this it was proposed that $\Gamma_{ann}(1S)$ = 0.3 KeV and the population of atomic 1S-level is 100%. From the new experimental data it follows that annihilation width of 1S-level is about 1 KeV and its population is less than 100% (from 60% [6] to 80% [5]). Taking into account these data the theoretical estimations [32] of γ-lines intensities should be diminished in 4 - 6 times. Hence the expected discrete lines should have a relative intensities in the diapason from 10^{-4} to 10^{-3}. The main interest is an investigation of γ-spectrum in the low energy range from 10 to 100 MeV since the binding energies of quasinuclear P-levels lie in this interval more probably. The predicted intensities of γ-lines show why for their observation an exclusive experiments are desirable.

The resonant $\bar{N}N$ states both narrow ($\Gamma \sim$ 10 - 20 MeV) and relatively wide ($\Gamma \sim$ 70 - 80 MeV) are hardly observed in the formation experiments without extraction of partial waves with definite quantum numbers. Let's to note that in our CCM calculations presented in this paper and in ref. [21] narrow D- and F-states in the region of S-meson are obtained. However the observation of such states in formation experiments needs the possibilities to make up the partial wave analysis. Another method to check narrow resonant states can be the production experiments in the case of clear reaction mechanism. It is necessary to note that in production experiments S-meson was observed independently by different experimental groups.

The polarization experiments for $\bar{N}N$ scattering could be also highly informative especially at very low energy where ρ-parameter (real-to-imaginary ratio for the forward elastic amplitude) has unusual (oscillating) behaviour.

The study of $\bar{p}p$-atom (investigation of relative intensities for K_α- and L_α-lines in the experiments at different pressure and shifts and widths of 1S- and 2P-levels) is a unique source of information on the scattering lengths for the states with different quantum numbers. The antiproton-nucleus scattering could be used as an independent source of essential information about the parameters of $\bar{N}N$-amplitude (in particular, extraction of $\rho_{\bar{p}n}$-parameter is possible now only from $\bar{p}$-nucleus scattering).

As for $\bar{\Lambda}\Lambda$ system these investigations are in the beginning at present. Observation of the clear effect of P-wave enhancement indicates on the existence of the spectrum of quasinuclear P-states in $\bar{\Lambda}\Lambda$-system. At present it is necessary to study an energy dependence of the total cross-section of $\bar{p}p \to \bar{\Lambda}\Lambda$ reaction, to measure more precisely the differential cross-sections and polarization characteristics. Direct observation of $\bar{\Lambda}\Lambda$-states (bound and resonant) is possible in the experiments with annihilation $\bar{p}p$ -- $\bar{K}K + n\pi$ in the mass range near $\bar{\Lambda}\Lambda$ threshold (such states should manifest themselves as a narrow meson resonances in $\bar{K}K + n\pi$ systems with expected production cross-sections of the order of several μb).

It is very interesting to study the processes of $\bar{p}p \to \bar{\Lambda}\Sigma + \Lambda\bar{\Sigma}$ and $\bar{p}p \to \bar{\Sigma}\Sigma$ near corresponding thresholds. It is theoretically possible to expect the existence of quasinuclear states in these systems [25] which should support the appearence of enhancement effects in the states with nonzero orbital momenta by the analogy with observation in the interactions of $\bar{\Lambda}$ and Λ.

Let's now emphasize once more that the aim of our calculations in the simplified CCM is the demonstration of the physical nature of observed phenomena. We did not try to obtain an exact theoretical description of the details of available experimental data.

The authors are sincerely grateful to K. Kilian and R. von Frankenberg for kind giving information about new experimental data.

Appendix 1

Here we show that the cross-section for square well potential in both channels as a function of annihilation coupling constant has an oscillating behaviour.

An interaction potential has the following form:

$$V = \begin{pmatrix} g_1 & \lambda g_0 \\ \lambda g_0 & g_2 \end{pmatrix} \qquad \text{at } r \le r_0$$

and

$$V = 0 \qquad \text{at } r \le r_0$$

(for simplicity the size of square well potentials put on the same). S-matrix element corresponding to the annihilation process can be written as [24]:

$$S_{12} = \frac{2\cdot(\zeta_1-\zeta_2)(\alpha_1\alpha_2 K_1 K_2)^{1/2}}{g(\rho_1,\rho_2)} \cdot e^{-i(\rho_1+\rho_2)}$$

where $\rho_i = (K_i r_0)/\sqrt{M_i}$, K_i is the momentum, M_i is the mass in channel i;

$$\zeta_i = e_i \operatorname{ctg} e_i;$$

$$\alpha_1 = e_1^2 - R_1^2 = R_2^2 - e_2^2 ; \quad \alpha_2 = e_2^2 - R_1^2 = R_2^2 - e_1^2 ;$$

$$e_{1,2}^2 = \tfrac{1}{2}\cdot(R_1^2 + R_2^2) \pm \tfrac{1}{2}\cdot[(R_1^2 - R_2^2)^2 + 4 g_0^2 r_0^4 \lambda^2]^{1/2} \quad ;$$

$$R_i^2 = (\rho_i^2 - g_i r_0^2) \quad ;$$

$$g(\rho_1,\rho_2) = i\rho_1(\zeta_1\alpha_1 - \zeta_2\alpha_2) + i\rho_2(\zeta_2\alpha_1 - \zeta_1\alpha_2) + (\alpha_1-\alpha_2)(\rho_1\rho_2 - \zeta_1\zeta_2) \, .$$

For a clearing of the formulae let's consider the case where λ is very large. In the limit of large :

$$e_1^2 \simeq g_0 \lambda r_0^2 \simeq \alpha_1 \quad ; \quad e_2^2 \simeq - g_0 \lambda r_0^2 \simeq \alpha_2 ;$$

$$i\ \mathrm{ctg}\, e_2 \simeq \mathrm{cth}|e_2| \simeq 1 \quad .$$

We take $\Lambda \equiv g_0 r_0^2 \lambda$, than

$$\sigma_{ann}(\lambda) \sim |S_{12}|^2 \sim \frac{\Lambda^3\ (\mathrm{ctg}\sqrt{\Lambda} + 1)^2}{\Lambda^3(\rho_1(\mathrm{ctg}\sqrt{\Lambda}-1)+\rho_2(\mathrm{ctg}\sqrt{\Lambda}+1))^2 + \Lambda^2(\rho_1\rho_2 + \Lambda^2\mathrm{ctg}\sqrt{\Lambda})^2} \ .$$

Hence we find the oscillating function of Λ with the period $T \simeq \pi^2$.

REFERENCES

1. W. Brückner et al., Phys. Lett. 166B (1986) 113
2. L.H. Johnston and D.A. Swenson, Phys. Rev. 111 (1958) 212
3. W. Brückner et al., Phys. Lett. 169B (1986) 302
4. L.M. Simons, Invited talk at IV LEAR Workshop, September 6-13 1987, Villars, Switzerland
5. L. Adiels et al., Preprint CERN-EP/86-154
6. S. Devons et al., Phys. Rev. Lett. 27 (1971) 1614
7. W. Brückner et al., Phys. Lett. 158B (1985) 180
8. L. Linssen et al., Nucl. Phys. A469 (1987) 726
9. H. Iwasaki et al., Nucl. Phys. A433 (1985) 580
10. V. Ashford et al., Phys. Rev. Lett. 54 (1985) 518
11. M. Cresti, L. Peruzzo and G. Sartori, Phys. Lett. 132B (1983) 209
12. O.D. Dalkarov and V.A. Karmanov, Nucl. Phys. A445 (1985) 579
13. S. Ahmad et al., Phys. Lett. 157B (1985) 333
14. T.P. Gorringe et al., Phys. Lett. 162B (1985) 71
15. O.D. Dalkarov and K.V. Protasov, JETP Lett. 44 (1986) 638
16. K. Kilian, Invited talk at XI International Conference "PANIC-87", April 20-24 1987, Tokyo, Japan;
    R. von Frankenberg, Invited talk at IV LEAR Workshop, September 6-13 1987, Villars, Switzerland;
17. I.S. Shapiro, Phys. Rep. 35C (1978) 129
18. O.D. Dalkarov and F. Myhrer, Nuovo Chimento 40A (1977) 152
19. B.O. Kerbikov et al., Preprint ITEP-61 (1978)
20. L.N. Bogdanova, V.E. Markushin and I.S. Shapiro, Sov. J.

Nucl. Phys. 30 (1979) 835

21. O.D. Dalkarov, I.S. Shapiro and R.T. Tyapaev, Preprint P.N. Lebedev Physical Institute №21 (1984)

22. I.S. Shapiro, Invited talk at XI International Conference "PANIC-87", April 20-24 1987, Tokyo, Japan;
I.S. Shapiro, Invited talk at IV LEAR Workshop, September 6-13 1987, Villars, Switzerland;
O.D. Dalkarov and K.V. Protasov, Pis'ma Zh.Eksp.Teor.Fiz 46 (1987) 261

23. M.M. Nagels, T.A. Rijken and J.J. de Swart, Phys. Rev. D20 (1979) 1633

24. R.G. Newton, Scattering Theory of Waves and Particles, (New York, 1966)

25. I.S. Shapiro and R.T. Tyapaev, Sov. Phys. JETP 59 (1984) 21

26. T.Kitagaki et al., AHL Proposal 368 (1973);
M.Maruyama and T. Ueda, Nucl.Phys. A364 (1981) 297

27. A.E. Kudryavtsev and V.E. Markushin, Preprint ITEP-179 (1985)

28. G. Bendiscioli et al., Nucl. Phys. A469 (1987) 669

29. J.-M. Richard, Proceedings of a Workshop on Physics at LEAR with Low-Energy Cooled Antiprotons, 1982, ed. U. Gastaldi and R. Klapisch (Pienum Press, New York and London, 1984) 83

30. M.G. Sapozhnikov, CERN-Report (1987)

31. G.Bardin et al., Preprint CERN-EP/87

32. O.D. Dalkarov, V.M. Samoilov and I.S.Shapiro, Sov. J. Nucl. Phys. 17 (1973) 566

33. F. Tabakin and R.A. Eisenstein, Phys. Rev. C31 (1985) 1857

34. M. Kohno and W. Weise, Phys. Lett. 179B (1986) 15

35. J.A. Niskanen, Helsinki preprint HU-TFT-85-28 (1985)

36. S. Furui and A. Faessler, Nucl. Phys. A468 (1987) 669

37. A.S. Clough et al., Phys. Lett. 146B (1984) 299;

K. Nakamura et al., Phys. Rev. D29 (1984) 349

38. T. Brando et al., Phys. Lett. 158B (1985) 505

39. $\bar{N}N$ and $\bar{N}D$ interactions. A compilation LBL-58 (1972)

40. R.P. Hamilton et al., Phys. Rev. Lett. 44 (1980) 1179

41. R. Bizzarri, A.E. Kudryavtsev and V.E. Markushin, Preprint Università di Roma N°892 (1987).

Table 1. Cut-off parameters for $\bar{N}N$ potential

$^{2S+1}L_J$ / I	$^1S_0$	$^3S_1$	$^1P_1$	$^3P_0$	$^3P_1$	$^3P_2$	$^1D_2$	$^3D_1$	$^3D_2$	$^3D_3$
0	0.55	0.50	0.70	0.55	0.72	0.72	0.62	0.62	0.63	0.62
1	0.60	0.50	0.64	0.68	0.72	0.67	0.62	0.52	0.54	0.62

Table 2. $\bar{N}N$ resonances in mass region 1700-1980 MeV

$^{2S+1}L_J$	I^G (J^P)	Mass, MeV	Total width, MeV	$\Gamma_{\bar{N}N}/\Gamma$
$^1P_1$	1^+ (1^+)	1840	70	--
$^3P_0$	1^- (0^+)	1855	75	--
$^3P_1$	1^- (1^+)	1870	75	--
	0^+ (1^+)	1800	35	--
$^3P_2$	1^- (2^+)	1870	85	--
	0^+ (2^+)	1860	70	--
$^1D_2$	1^- (2^-)	1975	35	0.3
$^3D_1$	1^+ (1^-)	1920	15	0.2
$^3D_2$	1^+ (2^-)	1930	20	0.3
	0^- (2^-)	1955	35	0.6
$^3D_3$	0^- (3^-)	1975	35	0.3

Table 3. Low energy S-wave parameters

$^{2I+1\ 2S+1}L_J$		Re a	Im a	ρ
$^{11}S_0$		- 1.92	6.10	
		- 2.45*	4.27*	
$^{31}S_0$		- 1.28	0.24	
$^{13}S_1$		- 0.34	0.34	
$^{33}S_1$		- 0.71	0.29	
S-wave	$\bar{p}p$	- 0.79	1.03	- 0.77
		- 0.86*	0.80*	- 1.08*
	$\bar{p}n$ (I=1)	- 0.85	0.28	- 3.07

Table 4. Low energy P-wave parameters

$^{2S+1}L_J$	Re A_p, $(GeV/c)^{-3}$	Im A_p, $(GeV/c)^{-3}$
$^1P_1$	84	64
$^3P_0$	71	105
$^3P_1$	- 4	96
$^3P_2$	53	130
P-wave	48	104

Figure captions

Fig. 1. Elastic differential cross-sections for $\bar{p}p$- and pp-scattering at the momentum of incident antiproton P = 287 MeV/c. The experimental data are taken from refs. [1,2].

Fig. 2. Charge-exchange differential cross-section at the momentum of incident antiproton P = 183 MeV/c. The experimental data are taken from ref. [3].

Fig. 3. Real-to-imaginary ratio for the forward elastic $\bar{p}p$-scattering amplitude as a function of incident antiproton momentum. The experimental data are taken from refs. [4,7-11].

Fig. 4. Total cross-section for $\bar{p}p \to \bar{\Lambda}\Lambda$ reaction as a function of incident antiproton momentum ($\mathcal{E}_{\bar{\Lambda}\Lambda}$ is the kinetic energy in $\bar{\Lambda}\Lambda$ c.m.s.). The experimental data are taken from ref. [16].

Fig. 5(a). Differential cross-section for $\bar{p}p \to \bar{\Lambda}\Lambda$ reaction at the energy $\mathcal{E}_{\bar{\Lambda}\Lambda}$ = 3.6 MeV. The experimental data are taken from ref. [16].

(b). The same at $\mathcal{E}_{\bar{\Lambda}\Lambda}$ = 0.6 MeV.

Fig. 6. Polarization of $\bar{\Lambda}(\Lambda)$ at $\mathcal{E}_{\bar{\Lambda}\Lambda}$ = 3.6 MeV. The experimental data are taken from ref. [16].

Fig. 7. Behaviour of annihilation cross-section σ_{ann} as a function of dimensionless annihilation constant for separable potential.

Fig. 8. The same for local potential.

Fig. 9. Total cross-section of $\bar{p}p$-interaction. The experimental data are taken from ref. [37].

Fig. 10. Annihilation cross-section of $\bar{p}p$-interaction. The experimental data are taken from ref. [38].

Fig. 11. Partial annihilation cross-sections for S-, P-, and D-waves.

Fig. 12. Elastic and charge-exchange cross-sections for $\bar{p}p$-interaction. The experimental data are taken from refs. [1,3,39,40].

Fig. 13. Relative partial cross-sections for the elastic $\bar{p}p$-scattering.

Fig. 14. The same as in fig. 1. Solid curve is the calculation from this work. Dashed curve is the same for $r_c(^{13}S_1) = 0.47$ fm, $r_c(^{33}S_1) = 0.60$ fm, $r_c(^{13}P_2) = 0.65$ fm.

Fig. 15. Relative partial annihilation cross-sections of $\bar{p}p$-interaction.

Fig. 16. The same as in fig. 3. Solid curve is the calculation from this work, dashed - taking into account $\bar{p}p \to \bar{n}n$ channel.

Fig. 17. Real-to-imaginary ratio for the forward elastic $\bar{p}n$ ($\bar{n}p$)-scattering amplitude. The experimental data are taken from ref. [28].

Fig. 18. The same as in fig. 4. Solid curve is the calculation from this work, dashed - S-wave contribution.

Fig. 19. The same as in fig. 5(a). Solid curve is the calculation from this work at $\varepsilon_{\bar{\Lambda}\Lambda} = 3.8$ MeV.

Fig. 20. The same as in fig. 6. Solid curve is the calculation from this work at $\varepsilon_{\bar{\Lambda}\Lambda} = 3.8$ MeV.

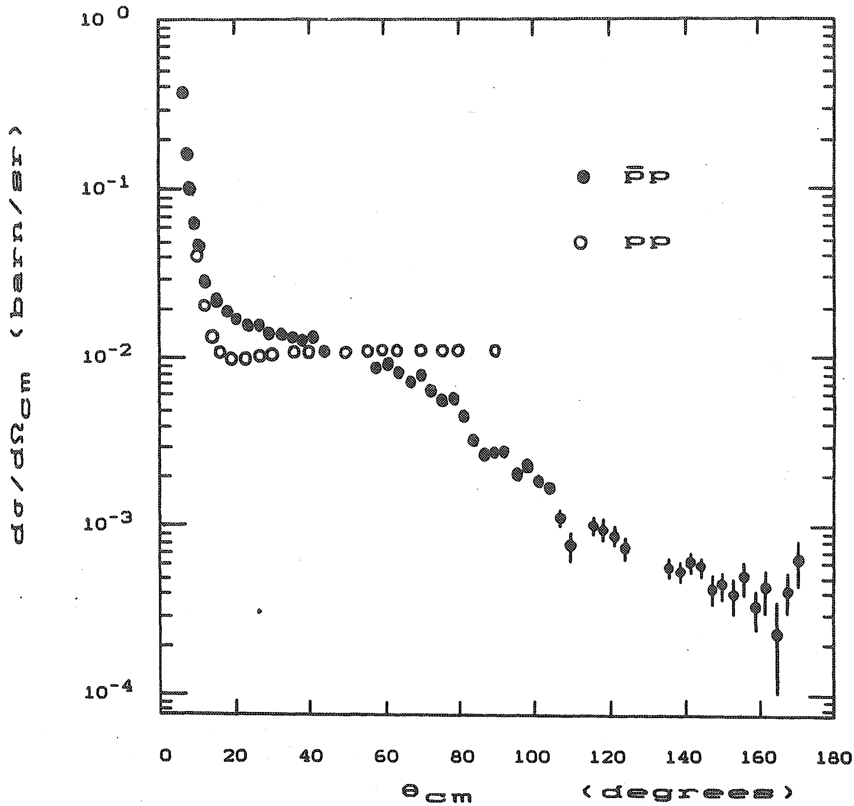
10 0
10⁻¹
10⁻²
10⁻³
10⁻⁴
dσ/dΩcm (barn/sr)
p̄p
pp
0
20
40
60
80
100
120
140
160
180
θcm (degrees)

Fig. 1

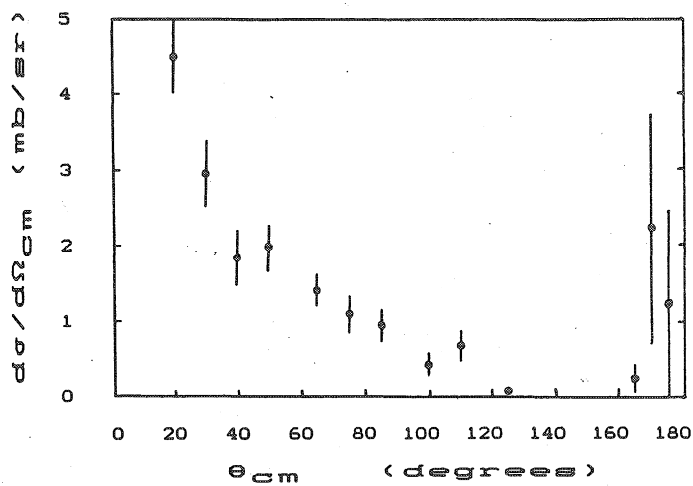
dσ/dΩcm (mb/sr)
5
4
3
2
1
0
0
20
40
60
80
100
120
140
160
180
θcm (degrees)

Fig. 2

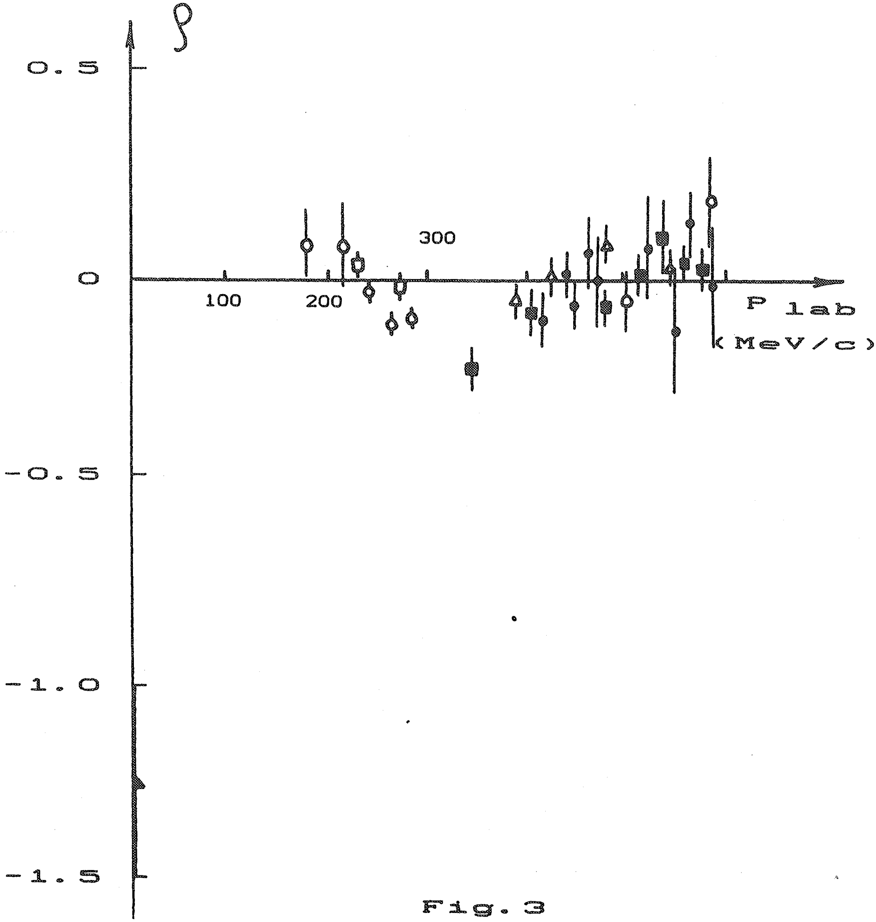

Fig.3

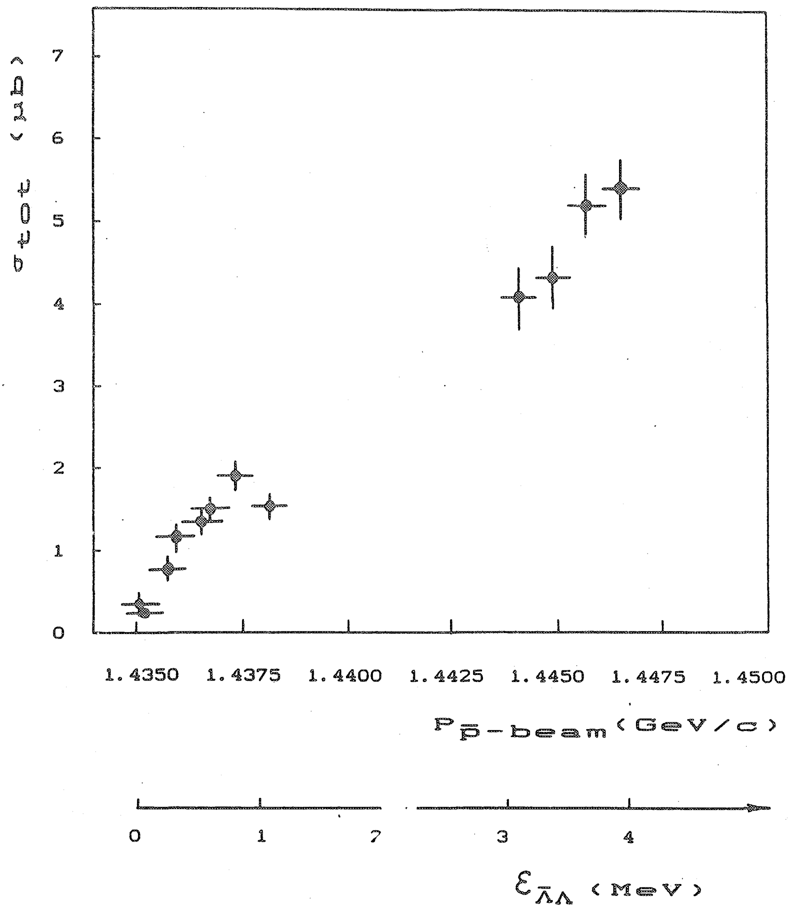
σ tot (μb)
7
6
5
4
3
2
1
0
1.4350
1.4375
1.4400
1.4425
1.4450
1.4475
1.4500
$P_{\bar{p}\text{-beam}}$ (GeV/c)
0
1
2
3
4
$\varepsilon_{\bar{\Lambda}\Lambda}$ (MeV)

Fig. 4

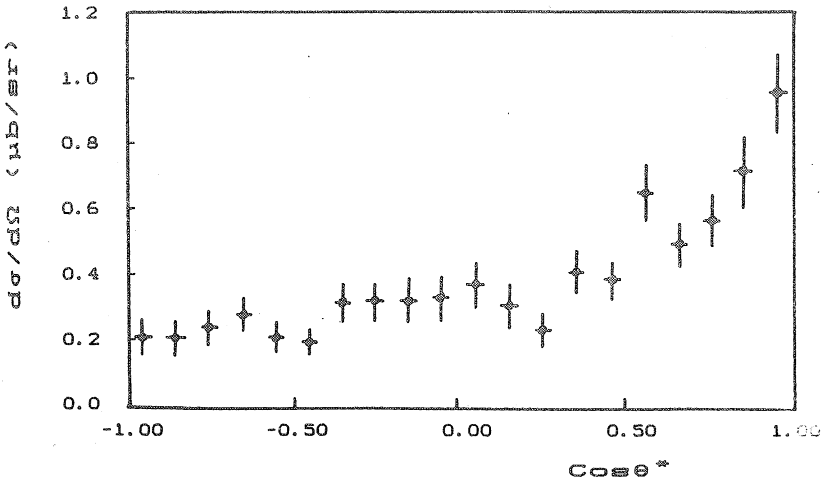
1.2
1.0
0.8
0.6
0.4
0.2
0.0
dσ/dΩ (μb/sr)
-1.00
-0.50
0.00
0.50
1.00
Cosθ*

Fig. 5(a)

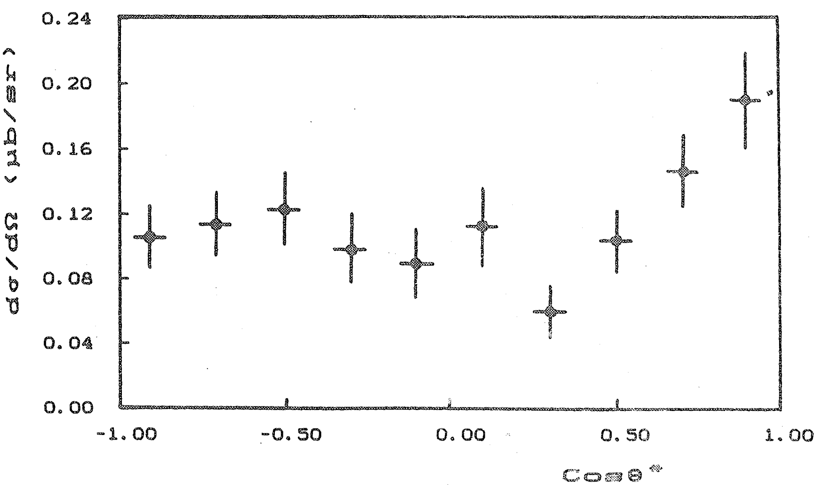
0.24
0.20
0.16
0.12
0.08
0.04
0.00
dσ/dΩ (μb/sr)
-1.00
-0.50
0.00
0.50
1.00
Cosθ*

Fig. 5(b)

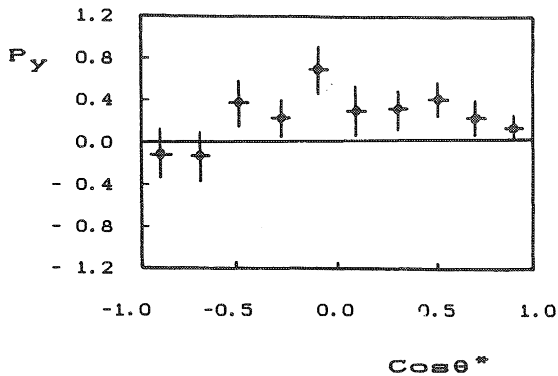

Fig. 6

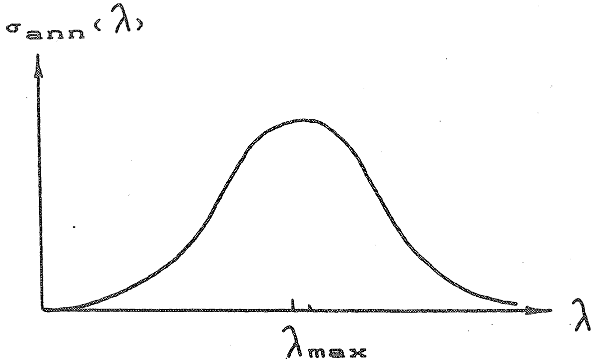

Fig. 7

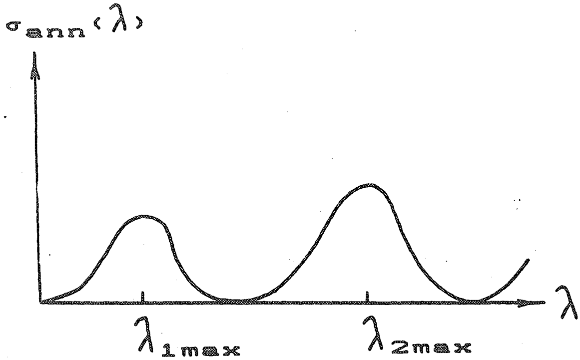

Fig. 8

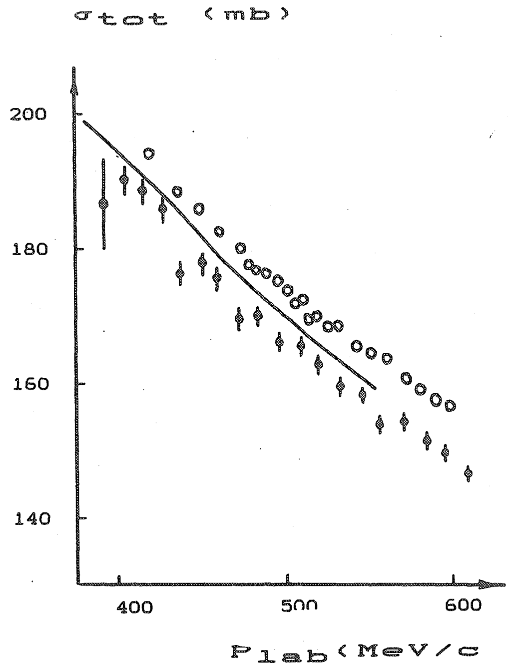

Fig. 9

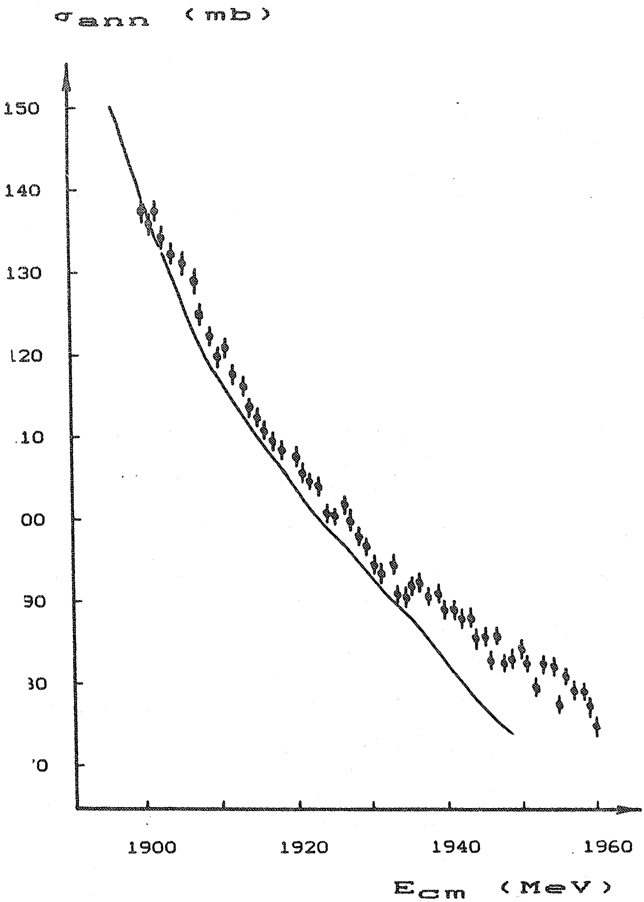
σann (mb)
150
140
130
120
110
100
90
80
70
1900
1920
1940
1960
Ecm (MeV)

Fig. 10

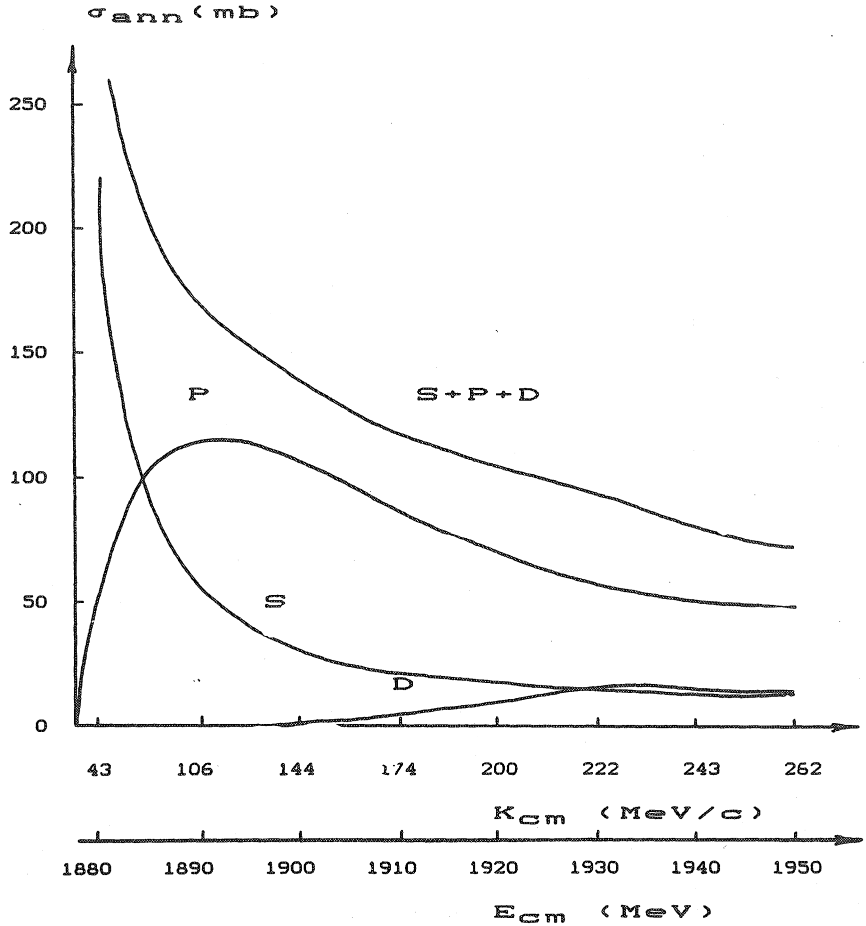
σann (mb)
250
200
150
100
50
0
P
S+P+D
S
D
43
106
144
174
200
222
243
262
Kcm (MeV/c)
1880
1890
1900
1910
1920
1930
1940
1950
Ecm (MeV)

Fig. 11

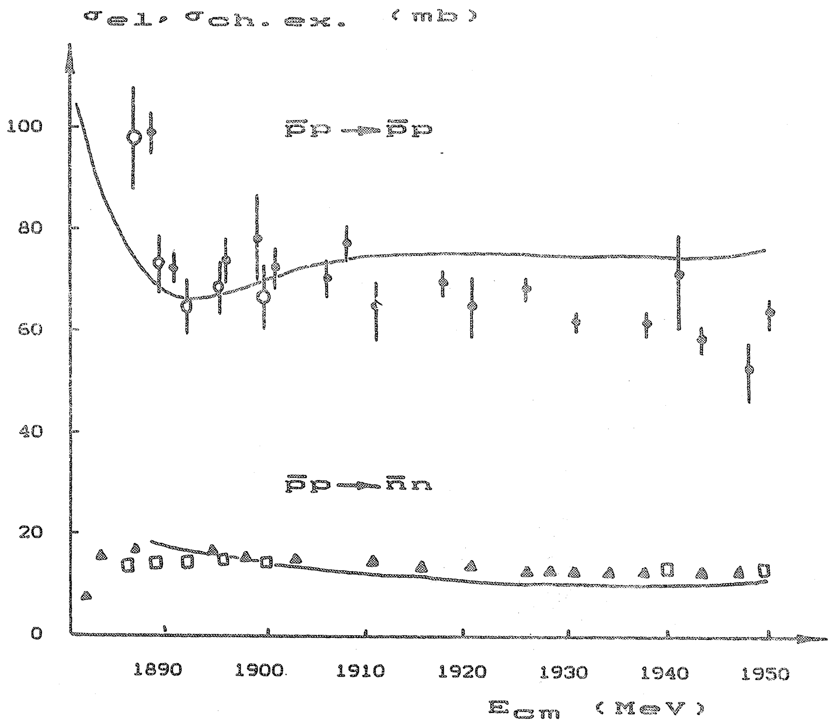

σel, σch. ex. (mb)
100
80
60
40
20
0
p̄p → p̄p
p̄p → n̄n
1890
1900
1910
1920
1930
1940
1950
Ecm (MeV)

Fig. 12

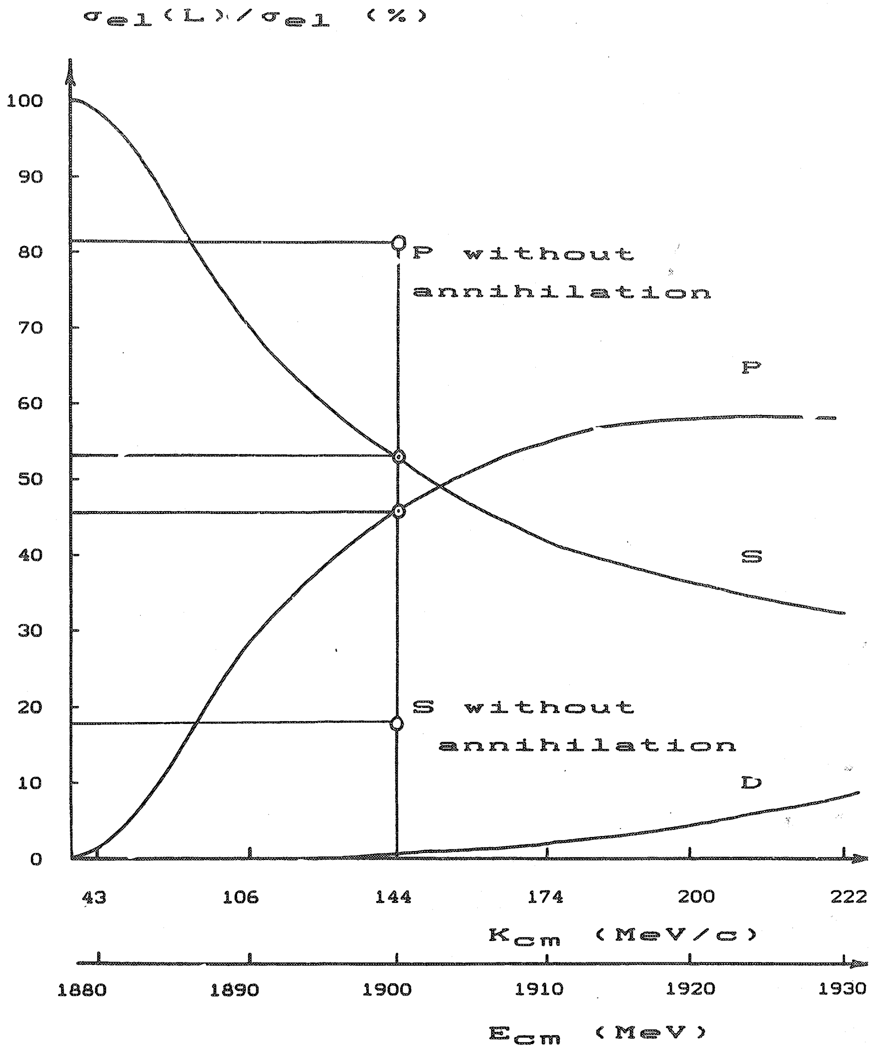
σel(L)/σel (%)
100
90
80
70
60
50
40
30
20
10
0
P without annihilation
P
S
S without annihilation
D
43
106
144
174
200
222
Kcm (MeV/c)
1880
1890
1900
1910
1920
1930
Ecm (MeV)

Fig. 13

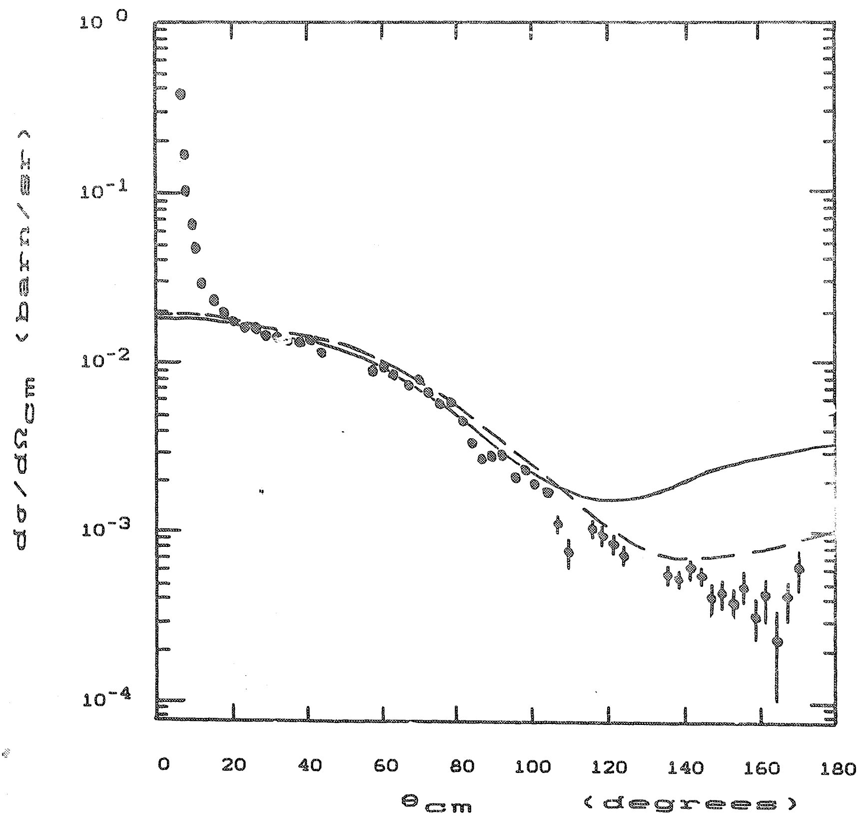
10 0
10-1
10-2
10-3
10-4
dσ/dΩcm (barn/sr)
0
20
40
60
80
100
120
140
160
180
θcm (degrees)

Fig. 14

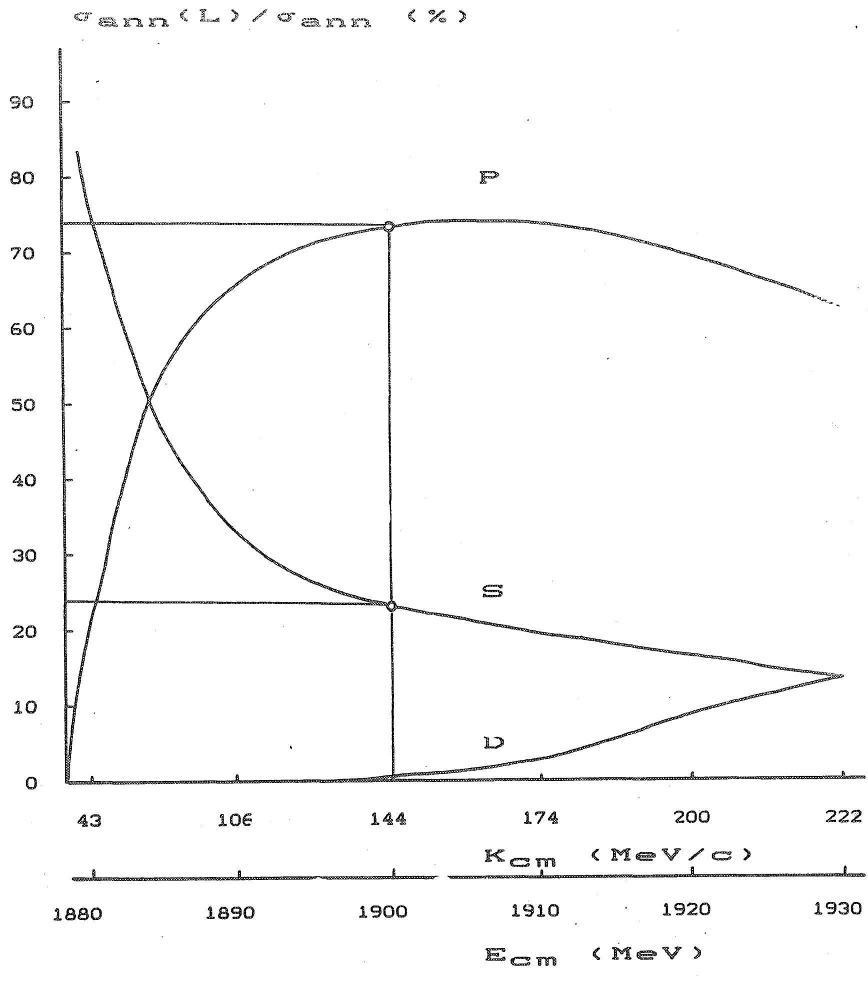
σann(L)/σann (%)
90
80
70
60
50
40
30
20
10
0
P
S
D
43
106
144
174
200
222
Kcm (MeV/c)
1880
1890
1900
1910
1920
1930
Ecm (MeV)

Fig. 15

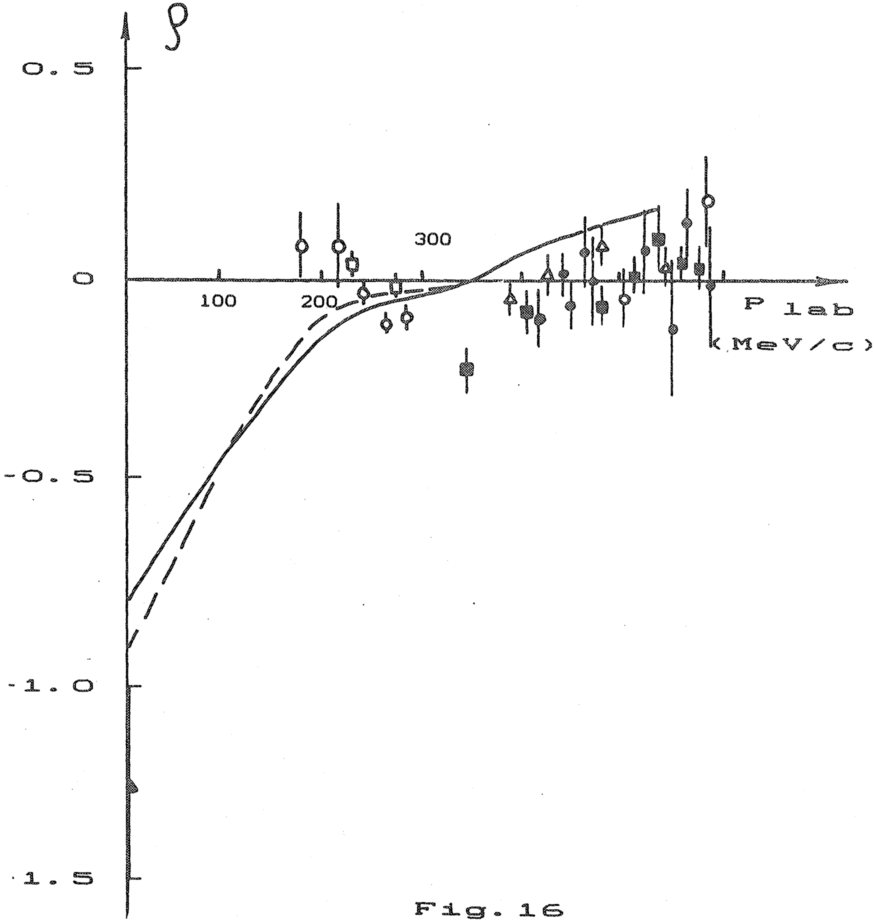

Fig. 16

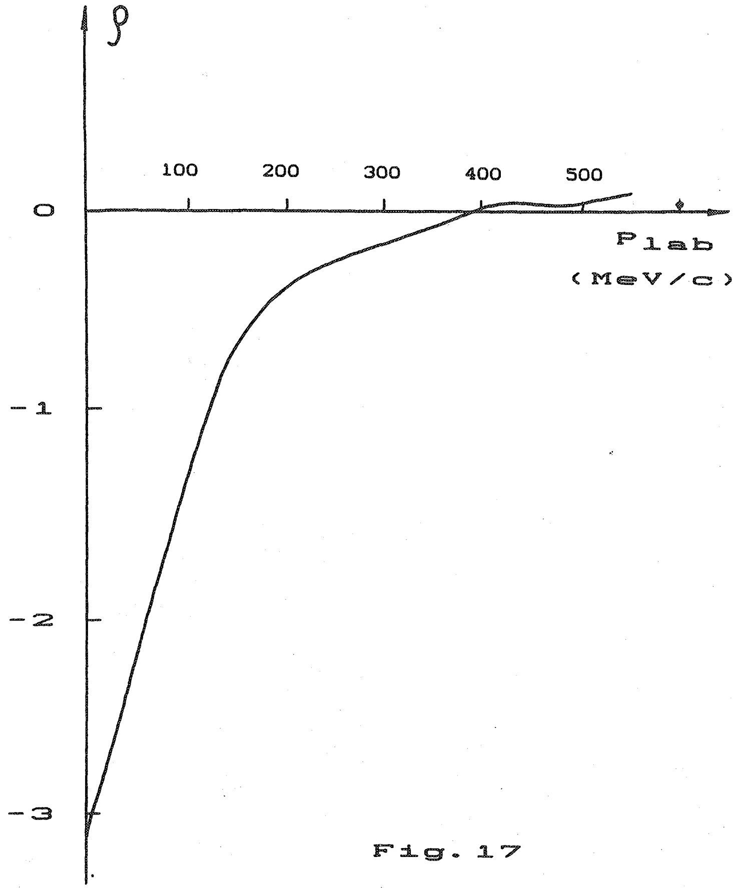

Fig. 17

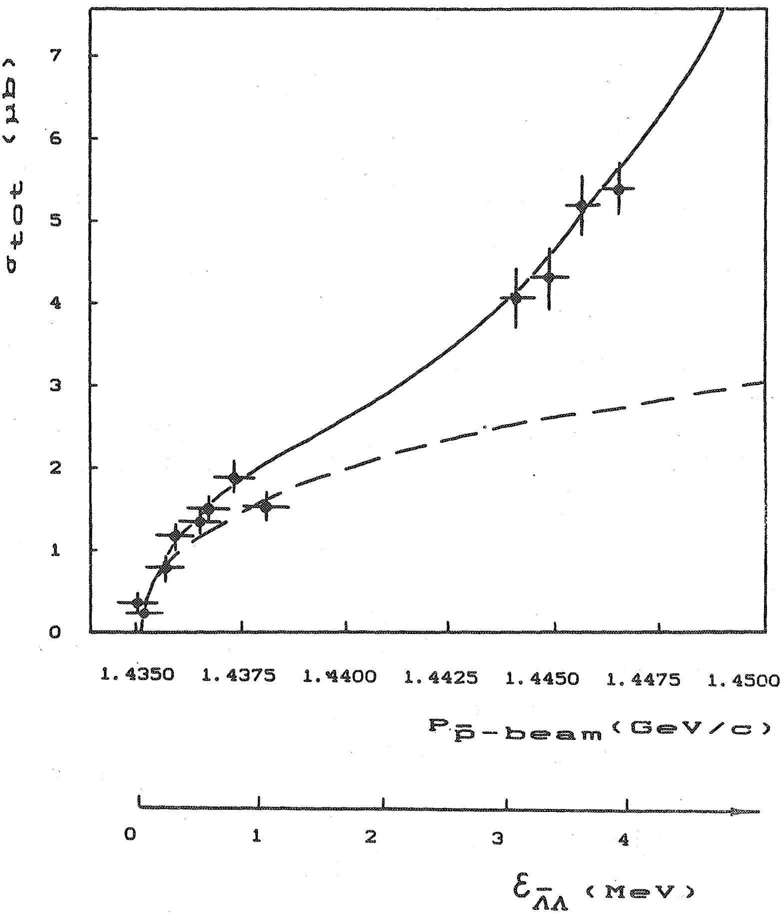
σtot (μb)
0
1
2
3
4
5
6
7
1.4350
1.4375
1.4400
1.4425
1.4450
1.4475
1.4500
$P_{\bar{p}-beam}$ (GeV/c)
0
1
2
3
4
$\varepsilon_{\bar{\Lambda}\Lambda}$ (MeV)

Fig. 18

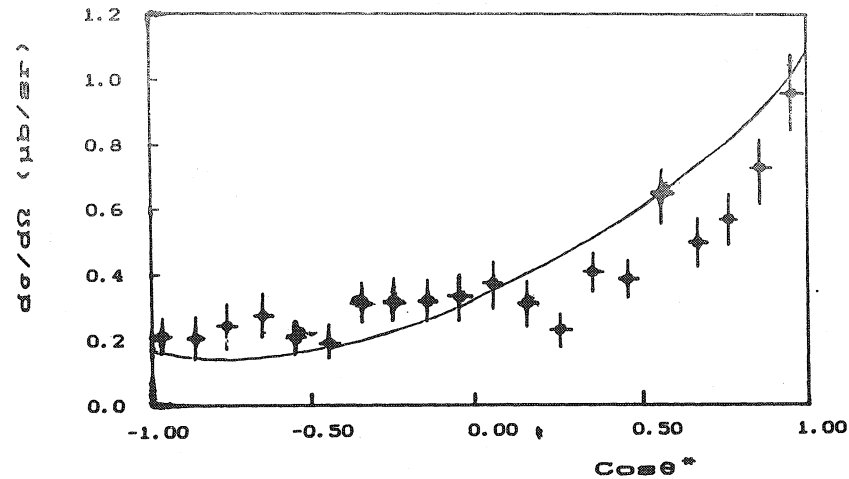
1.2
1.0
0.8
0.6
0.4
0.2
0.0
dσ/dΩ (μb/sr)
-1.00
-0.50
0.00
0.50
1.00
Cosθ*

Fig. 19

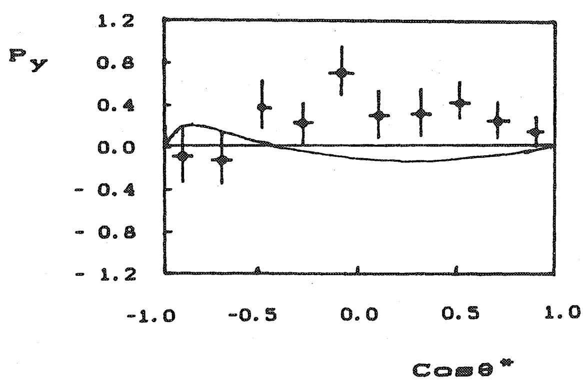
Py
1.2
0.8
0.4
0.0
- 0.4
- 0.8
- 1.2
-1.0
-0.5
0.0
0.5
1.0
Cosθ*

Fig. 20

Препринты Физического института имени П.Н. Лебедева АН СССР рассылаются научным организациям на основе взаимного обмена.

Наш адрес: 117924, Москва В-333, Ленинский проспект, 53

Preprints of the P.N. Lebedev Physical Institute of the Academy of Sciences of the USSR are distributed by scientific organizations on the basis of mutual exchange.

Our address is: USSR, 117924, Moscow B–333, Leninsky prospect, 53

Т – 22823. Подписано в печать 22. 12. 1987 г.
Заказ № 79. Тираж 100 экз. П.л. 3,6.

Отпечатано в Отделе научно-технической информации ФИАН СССР
Москва, В-333, Ленинский проспект, 53